

Rupture and coalescence in two-dimensional cellular automata fluids

Marek Cieplak

Institute of Physics, Polish Academy of Sciences, 02-668 Warsaw, Poland
(Received 12 August 1994; revised manuscript received 1 November 1994)

A two-dimensional, two-color, nonlinear, Galilean invariant, Boltzmann cellular automaton is used to study rupture and coalescence processes in two fluid systems. A Lyapunov distance is introduced to characterize the dynamics of rupture, and its dependence on the parameters of the system, such as the coefficient of the surface tension, is studied. Systematic trends are obtained. A comparison to molecular dynamics studies is made. Coalescence is studied in the context of a droplet in a background fluid falling in a gravitational field to the bottom of a container. Three cases have been studied: a "bare" wall, a shallow liquid of the same kind as the droplet, and a deeper liquid. In each case, detailed momentum and density fields are obtained and compared.

PACS number(s): 47.11.+j, 02.70.Ns, 05.50.+q

I. INTRODUCTION

The rupture and coalescence of fluid interfaces are challenging problems [1] since the phenomena occur at two disparate length and time scales. While the bulk fluid is conveniently treated within the framework of continuum fluid mechanics, the interface is characterized by lengths measured in molecular diameters and local motion on time scales below the picosecond range. Recent studies [2,3] using molecular dynamics simulations have allowed for an attack of such problems and have yielded detailed microscopic information not easily available by other means. However, the inherent limitation of the small sizes of systems accessible with present day computers has not permitted the determination of meaningful Navier-Stokes fields. The conventional continuum physics methods, on the other hand, are expected to fail when the processes considered take place at length scales that are approaching molecular distances.

In this paper, we describe the results of studies of the rupture and coalescence of liquid interfaces using a Boltzmann cellular automata (BCA) technique [4]. It is well known that the cellular automata model [5,6,14,15] reproduces hydrodynamical behavior at coarse-grained length and time scales. The Boltzmann approach incorporates an averaging over many possible simultaneous configurations, leading to an avoidance of noise problems commonly associated with Boolean cellular automata [7]. Interfaces are created in BCA by allowing for two fluids and kinetic rules that lead to phase separation. Indeed, our BCA has two parameters β_1 and β_2 that allow for control of the interfacial tension and width, respectively. Our model is Galilean invariant due to the presence of a judiciously chosen number, n_0 , of rest particles is fully nonlinear, and allows for arbitrary densities and color ratios in the lattice sites. The present studies are all in two dimensions; an extension to three dimensions is possible but we have not developed the machinery yet to carry this out. The interfacial tension in the BCA is created us-

ing kinetic rules that incorporate like color attraction and unlike color repulsion. Earlier studies have shown that many of the features of the interfaces of real fluids are captured adequately by our model. Further, the Boltzmann approach provides for a large signal to noise ratio and allows one to extract meaningful velocity and density fields. At the very least, our studies provide new insights into the complex problems of interfacial processes within the framework of a toy kinetic model.

This paper is organized as follows. In Sec. II we outline the BCA model and the way the interfaces are introduced. In Sec. III we present results of systematic studies of a thread rupture and validate our approach by molecular dynamics studies of rupture in two dimensions. Finally, in Sec. IV we discuss the coalescence of a droplet impinging upon a wall.

II. BOLTZMANN CELLULAR AUTOMATA MODEL

In this paper, we use a variant of the BCA technique for studying a pair of fluids in two dimensions with a desired degree of miscibility. Our method [4] is closely related to that of Gunstensen *et al.* [7]:

(i) Our system is Galilean invariant [8]; the vortex advection velocity matches the interfacial velocity.

(ii) The method adopts the Boltzmann approach. The conventional Boolean automata require spacial coarse-graining and averaging over long periods of time, which make them hard to use for monitoring dynamical situations. In the Boltzmann approach the individual event collision rules correspond to one of the set of rules suggested by Frisch, Hasslacher, and Pomeau [9] (FHP II) but one considers ensembles of microscopic configurations by ascribing probabilities of occupation to each of the discrete velocity states.

One difference of our approach from that of Ref. [7] is that the collision operator of our automaton is fully nonlinear; the kinetic equation that governs the time evolution of the system does not rely on the linearization in the density difference away from a steady state. Our

prescription for having fluids of two colors follows the approach of Rothman and Keller [6], but it improves on it by introducing two microscopic parameters β_1 and β_2 , which allow for a flexible control of the surface tension (by half an order of magnitude) and interface thickness, respectively. The method of Ref. [6] relies on a one-parameter control of the interface and involves a maximization of the scalar product of the color gradient with the color momenta when redistributing the color after a color-blind collision. In our recoloring scheme the difference between the densities of the two colors along the α th direction depends continuously on the angle ϕ_α between the α axis and the color gradient.

Our coloring scheme involves two steps, the first of which is like that in Ref. [7]: we determine the color gradient vector \vec{g} at each node and increase the total state density along the axis defined by the color gradient with a decrease in the density in a direction perpendicular to the axis,

$$f'_\alpha = f_\alpha + \beta_1 |\vec{g}| \cos 2\phi_\alpha, \quad (1)$$

where f_α refers to the initial state density, f'_α is the density after the redistribution, and ϕ_α is the angle between the α th axis (on a triangular lattice, α takes on one of six values) and \vec{g} . Note that $f_\alpha = r_\alpha + b_\alpha$, where r_α and b_α are the red and blue state densities, respectively. Our second step for the reassignment of colors is according to the equations

$$r'_\alpha = \frac{R_t}{R_t + B_t} f'_\alpha + \beta_2 \frac{R_t B_t}{(R_t + B_t)^2} \cos \phi_\alpha, \quad (2)$$

$$b'_\alpha = \frac{B_t}{R_t + B_t} f'_\alpha - \beta_2 \frac{R_t B_t}{(R_t + B_t)^2} \cos \phi_\alpha, \quad (3)$$

for the moving states ($\alpha = 1, 2, \dots, 6$), and

$$r'_o = \frac{R_t}{R_t + B_t} f'_o, \quad (4)$$

$$b'_o = \frac{B_t}{R_t + B_t} f'_o, \quad (5)$$

for the states at rest, where R_t and B_t refer to the total red and blue densities at a node (r and b stand for red and blue, respectively). The parameters β_1 and β_2 typically take on values of the order of 0.001 and 0.2. Our prescription for the introduction of immiscibility avoids an abrupt interface whose properties would be sensitive to its orientation with respect to the underlying lattice.

We have determined that the coefficient of the surface tension, γ , is proportional to β_1 and substantially independent of β_2 . On the other hand, the interface thickness has been found to be proportional to β_2^{-1} and not to depend on β_1 (for $\beta_1 = 0.001$ and $\beta_2 = 0.25$ it is of the order of three lattice spacings). This two parameter control of the interface properties is reminiscent of the classical approach to the interfacial properties of nonuniform systems [4] (for example, van der Waals fluids).

The introduction of the two color method to study two fluids also allows one to take into account the wetting

properties of the system in the vicinity of a wall. Following the prescription of Ref. [6] one may obtain desired wetting properties by setting the color content of the walls to the appropriate value. As usual, we employ bounce-back boundary conditions at the wall in order to impose a no-slip condition. We have found that the contact angle behaves approximately linearly with the relative color content of the wall. We now proceed to the studies of rupture and coalescence within our model.

III. RUPTURE

The Rayleigh liquid thread instability can be studied in the following arrangement. Consider a two-dimensional box of $L \times M$ sites. Due to the hexagonal lattice used in the FHP II model, the corresponding linear sizes are $L a$ and $\sqrt{3}/2 M a$, where a is the lattice constant. Unless stated otherwise, we take $L = 64$ and $M = 32$. Periodic boundary conditions are applied in all directions. In the center of the box we place a "ribbon" of the red colored fluid parallel to the L axis. The ribbon is w layers thick; typically $w = 6$. All of the remaining sites are populated with the blue particles, and each site is thus either totally red or totally blue. We study the Galilean invariant case when each velocity state is initially occupied with the probability $f_\alpha(\mathbf{r}, t) = \frac{1}{3}$ and $n_0 = 18$ [the density at a site is $(6 + n_0)/3$].

We let the system evolve until, reaching a steady situation in which the initially abrupt interface develops a thickness and the familiar hyperbolic tangent, the red and blue densities are obtained. This happens typically within 800 time steps. We store the total red, $R_t(\mathbf{r}, 0)$, and blue, $B_t(\mathbf{r}, 0)$, densities at each site located at \mathbf{r} at time $t = 0$.

The system is then perturbed sinusoidally at the two lines that were the boundaries of the red color in the initial state with the abrupt interface. In each state of a site belonging to the boundary lines the red color densities acquire an additive perturbation $\delta R = A \sin(kx)$, where $k = 2\pi/\lambda$, with λ usually equal to L , and x is the distance along the L axis. The blue densities of these sites are perturbed by $-\delta R$ so that the total state probabilities f_α remain unchanged. If the amplitude A is sufficiently large or λ is sufficiently big, the ribbon will evolve to acquire a circular shape in order to minimize the interface. This entails the thinning of the ribbon and subsequent rupture of some location x_c , followed by an evolution to a circular shape. As a working criterion of determining the rupture time T_r , we chose a situation in which along at least one line, parallel to the M axis, the total red content on each site was less than 10% of the total density.

In order to monitor the onset of the instability quantitatively we introduce a Lyapunov distance

$$d^2 = \frac{\sum_{\mathbf{r}} \{ [R_t(\mathbf{r}, t) - R_t(\mathbf{r}, 0)]^2 + [B_t(\mathbf{r}, t) - B_t(\mathbf{r}, 0)]^2 \}}{\sum_{\mathbf{r}} \{ [R_t(\mathbf{r}, t) + R_t(\mathbf{r}, 0)]^2 + [B_t(\mathbf{r}, t) + B_t(\mathbf{r}, 0)]^2 \}}, \quad (6)$$

where $R_t(\mathbf{r}, t)$ and $B_t(\mathbf{r}, t)$ are the total red and blue densities at site \mathbf{r} at time t as measured from the instant the

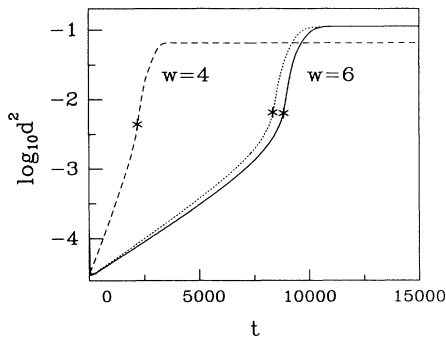


FIG. 1. Logarithm of the square of the Lyapunov distance d^2 versus time for $L=64$, $M=32$, $\lambda=64$, and $w=6$ (solid line) or 4 (dashed line). The dotted line corresponds to $L=256$ and $w=6$ with λ remaining at 64. In this case four circles are formed from a single ribbon. The interface control parameters are $\beta_1=0.001$ and $\beta_2=0.25$. The asterisk marks the value of the rupture time T_r . The amplitude A is equal to 0.03. For $w=8$ there is no rupture taking place at these values of the parameters.

perturbation is applied. The normalization used in the definition of d^2 is chosen so that in a totally decorrelated state d^2 would be of order 1. A growth of d^2 indicates an onset of instability, whereas a steady decay to zero signals stability.

A typical behavior of d^2 versus time for a perturbation that leads to instability is shown in Fig. 1. After an initial transient decay, about 100 time steps long, d^2 grows exponentially. Around the rupture time, indicated by the asterisks, d^2 undergoes a sudden rise and then levels off, indicating a new equilibrium with a circle of red liquid present.

Generally, the larger the ribbon width, the longer the T_r . For $A=0.03$, $\lambda=L=64$, T_r is 2200 and 8850 for $w=4$ and 6, respectively. Changing w to 8 leads to a rapid decay of d^2 , indicating stability (no rupture occurs within 15 000 time steps, even with $A=0.06$ in this case).

The sensitivity of the rupture process to the amplitude A is demonstrated in Fig. 2. The growth exponent for d^2 is seen to be essentially A independent but the amplitude of the growth law increases with A rapidly. The presence

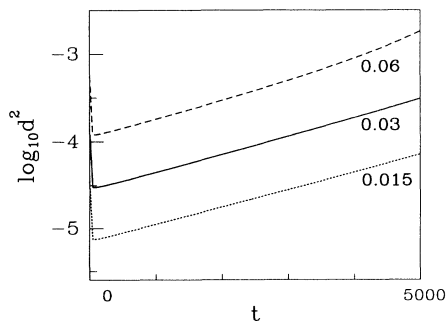


FIG. 2. Sensitivity of d^2 to the amplitude of the perturbation for $\lambda=L=64$, $M=32$, $w=6$, and β_1 and β_2 as in Fig. 1. The values of the amplitude are indicated next to the data lines.

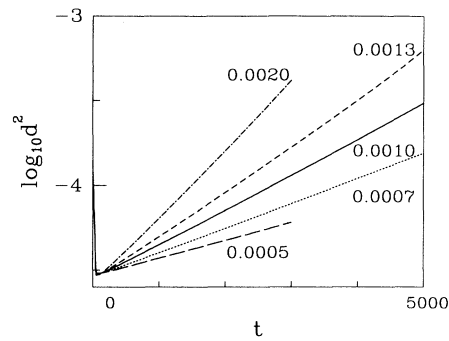


FIG. 3. d^2 versus t plots for various values of the surface tension as controlled by β_1 . The values of β_1 are indicated next to the data lines. The values of other parameters are as in Fig. 2 with $A=0.03$.

of the sensitivity to A makes it difficult to make systematic studies of the rupture time dependence on L , since “equal amounts of perturbation” would have to be defined first. We just point out, as an example, that for $w=6$, $A=0.03$, $\beta_1=0.001$, $\beta_2=0.25$ the perturbations with $\lambda=L$ induce rupture for L larger than or equal to 44, whereas smaller wavelengths do not generate any instability. For $w=2$ and 4 all λ 's larger than or equal to 16 (smaller values were not studied) gave rise to instability. On the other hand, for $w=8$, wavelengths even as long as 128 still do not yield rupture.

We now consider the dependence of the onset of instability on the interface control parameters β_1 and β_2 . Figure 3 shows d^2 for various values of β_1 , which is proportional to the surface tension coefficient. The growth rate exponent is roughly linear in β_1 : the stronger the surface tension, the sooner rupture takes place.

Similarly, the wider the interface, the easier it is to induce rupture. Thus the growth rate exponent increases with β_1^{-1} linearly, as demonstrated in Fig. 4.

A linear stability analysis, in three dimensions, due to Rayleigh [10] has led to the following expression for the growth rate of sinusoidal perturbations of wave number k on a cylinder of diameter d :

$$\omega(k) = \gamma [1 - (kd/2)^2] / 3\eta d, \quad (7)$$

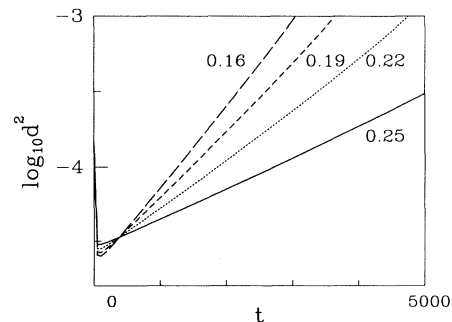


FIG. 4. d^2 versus t plots for various values of the interface width as controlled by β_2^{-1} . The values of β_2 are indicated next to the data lines. The values of other parameters are as in Figs. 2 and 3 with $A=0.03$ and $\beta_1=0.001$.

where η is viscosity and γ is the coefficient of the surface tension. The criterion indicates that for a given d the wavelength, which is limited by the system size, must be big enough to ensure a positive ω , i.e., rupture. Our results agree qualitatively with the existence of a critical wavelength, with the proportionality of ω to γ , and the lack of the dependence of the growth rate on the amplitude of the perturbation.

In the following we provide quantitative pictures of the velocity fields and the density patterns in the process of rupture. We focus on a system with the parameters $\lambda=L=64$, $M=32$, $A=0.03$, $\beta_1=0.001$, $\beta_2=0.25$, and $w=6$. Periodic boundary conditions are applied in all directions. Figure 5 shows the time evolution of the system in eight representative snapshots. The corresponding time is indicated at the top of each set of three panels. The lengths of the arrows are proportional to the momenta, whereas the sizes of the bars are proportional to the red density. The time is measured in BCA time step units with the rupture event defined to be at $t=0$. In this particular example, the perturbation is applied immediately after an abrupt interface is set up and not after a period of equilibration. T_r is equal to 7279 in this case. Each set of three panels shows, from top to bottom, the momentum field of the red (ribbon) fluid, the density field of the surrounding blue fluid, and the momentum field of

the blue fluid. Generally, next to the interface, the blue momentum should be roughly parallel to the red momentum in order to avoid viscous stresses.

The evolution to a steady state lasts for about 9000 time units. The initial configuration corresponds to a ribbon in the middle. In the final steady situation the red density forms a circle. There would be n circles if L were equal to $n\lambda$. Even though the Lyapunov distance grows right from the beginning the noticeable effects of the perturbation affecting the system appear only 5000–6000 units later: the red density develops a thinning and, in another place along the ribbon, the red momentum reverts itself. The subsequent actual rupture of the distorted configuration takes place fast—within several hundred steps. The red momentum becomes highly structured, and it alternates its direction in a steplike fashion. Furthermore, the red momentum becomes substantial, even relatively far away from the original location of the ribbon. By contrast the blue momentum behaves much smoother and all modifications are restricted to the rupturing tip. Just after the rupture point a rapid folding to a circle—through a bean shaped object—takes place. Again the blue fluid acts more passively than the red one and the blue momentum is less structured.

Rupture of real fluids may or may not belong to the “universality class” of the BCA. However, it seems likely

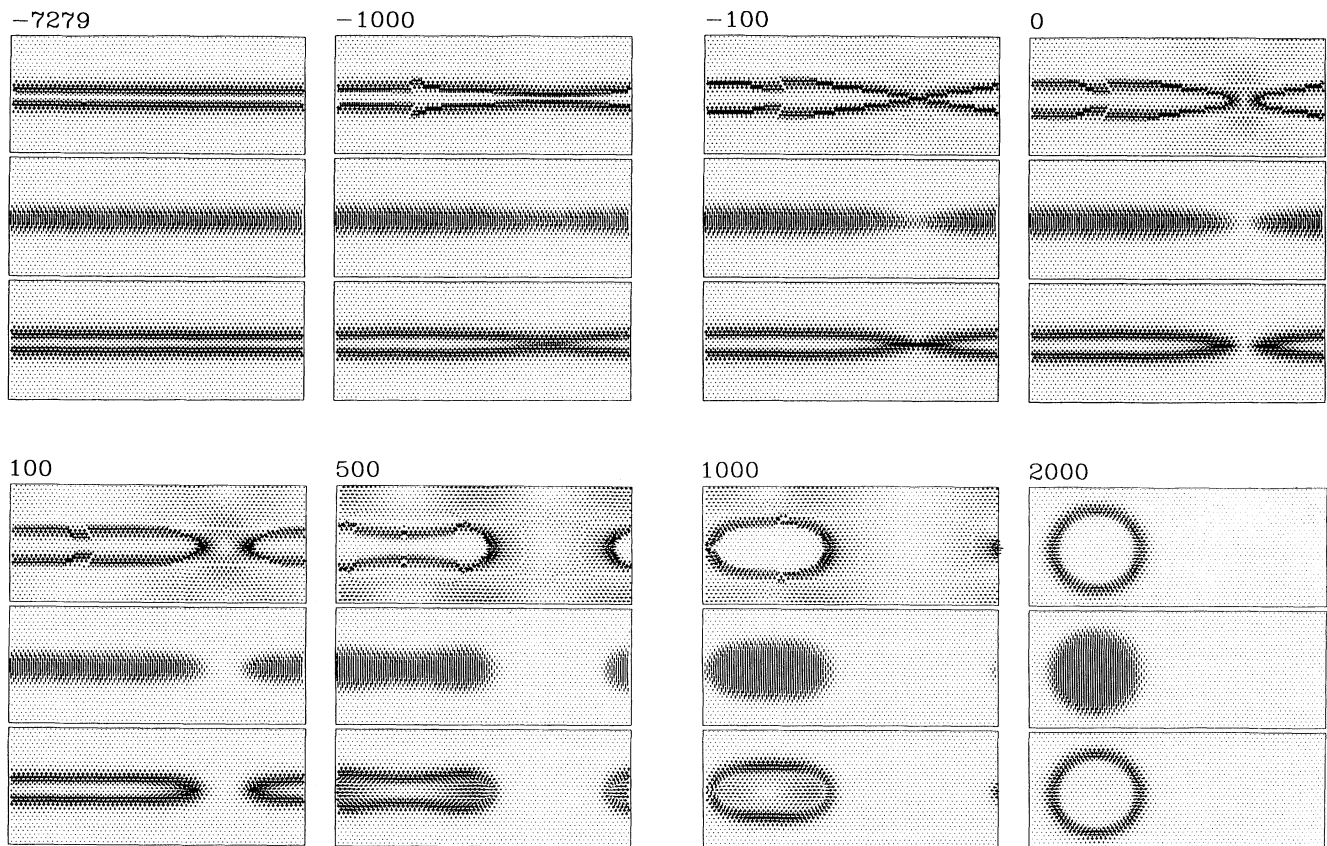


FIG. 5. The dynamics of rupture as described in the text. The numbers at the top of each threefold set of panels indicate time measured away from the rupture point T_r .

that the overall behavior the two fluids ought to be qualitatively as shown in Fig. 5.

Our BCA results are restricted to two dimensions. Would two-dimensional filaments of real fluids indeed undergo rupture? A positive answer to this question appears to be suggested by our molecular dynamics studies of the problem. Rupture in three dimensions in systems of Lennard-Jones atoms has been studied by Koplik and Banavar [3]. Here, we follow their general approach but we confine the atoms to a plane. The confinement is implemented like in Ref. [11], i.e., by placing the atoms next to an attracting wall, except that we do not take corrugation of the wall potential into account. The potential due to the wall has a sharp minimum at a position determined by the wall parameters [12]. The interatomic potential is of the Lennard-Jones form $V(r)=4\epsilon[(\sigma/r)^{12}-(\sigma/r)^6]$.

We consider 200 atoms that emulate krypton, i.e., we take $\epsilon/k_B=202$ K and $\sigma=3.57$. The characteristic time scale of the atomic motion is $t_0=\sqrt{m\sigma^2/\epsilon}=2.5$ ps, where m is the atomic mass. The temperature is taken to correspond to the liquid nitrogen, which makes the atomic movements essentially two dimensional.

Figure 6 shows what happens to the atomic velocities after the atoms are arranged in five rows, separated by 1.21σ , to form a "ribbon" of length 48.5σ (other densities yield a similar behavior). The initial velocities are randomly directed. The evolution is monitored for 5044 ps. The rupture, analogous to the one observed in Ref. [3], is taking place almost immediately and a well developed gap is present already at 252 ps. Thus rupture does take place. What follows is a steady formation of two, in this case, irregular globular structures. Obtaining

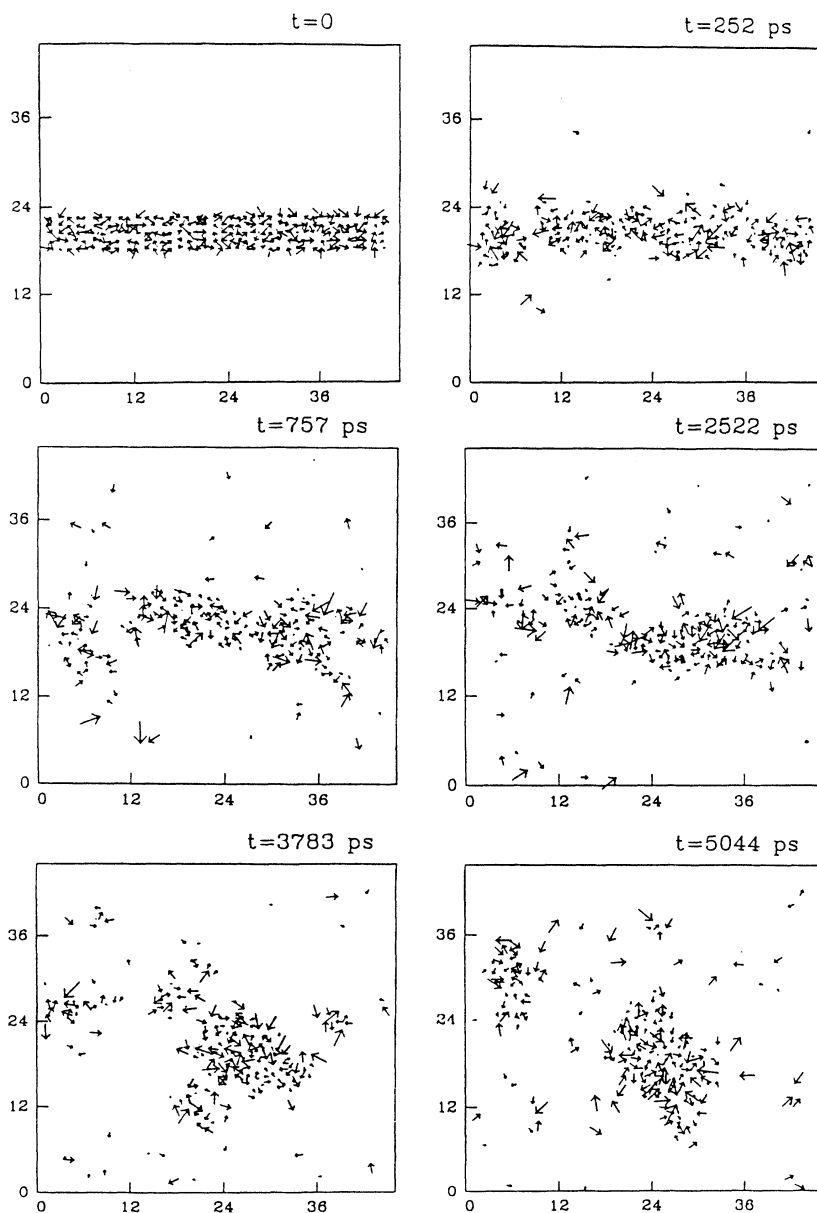


FIG. 6. Molecular dynamics studies of rupture next to a confining wall: snapshots of the particles' velocities at instances indicated. The x and y coordinates on the axes are in units of σ .

this evolution took about a week of CPU on a Sun workstation, and averaging over hundreds of starting configurations to determine the Navier-Stokes fields, free of noise, was clearly impossible, even by working only with 200 molecules. This indicates the power to harness from the cellular automata approaches: the fully averaged momentum and density fields corresponding to Fig. 5 were obtained in several hours of CPU on the same machine.

The major limitation of the BCA method, however, is that it does not capture the molecular level physics correctly and at this level the results acquire a merely qualitative character. A linear stability analysis due to San Miguel, Grant, and Gunton [13] indicates that hydrodynamics does not give rise to the Raleigh stability in two dimensions. Our BCA studies did not yield any rupture if the width of the filament was too wide, like eight layers or more, which indicates agreement with the hydrodynamic behavior. On the other hand, the molecular dynamics results indicate a molecular mechanism for the occurrence of rupture. Thus the BCA results for small values of w qualitatively agree with the microscopic nature of the phenomenon but no details are expected to be realistic.

IV. COALESCENCE

We now consider another two-fluid situation in which a hydrodynamic description must break down at some point of evolution—that of fluid coalescence. Specifically, we place a droplet of a red fluid at the top of a rectangular cavity, as shown in Fig. 7. The system size is 64×64 (we have tried a range of sizes and the behavior is qualitatively the same). The cavity is filled with a blue fluid, so the surface tension makes the droplet circular (the radius is about nine lattice constants). The red fluid is assumed to be heavier than the blue one so the gravity forces g can be taken to act exclusively on the red fluid, as an approximation. The gravity accelerates the droplet down and the viscous drag saturates the velocity of the fall at a constant and g -dependent value. There is a bottom wall in the cavity so the droplet must eventually impact normally on it and, through several stages of transformations, cease to be an independent droplet. The blue and red fluids are of the same viscosity and the fluid in the droplet and the one at the bottom are of the same kind. On all walls, bounce-back boundary conditions are imposed.

The effects of gravity are mimicked by adding $gy(\alpha)$ to the red density r_α , where $y(\alpha) = \pm 1$ or $\pm \frac{1}{2}$, depending on

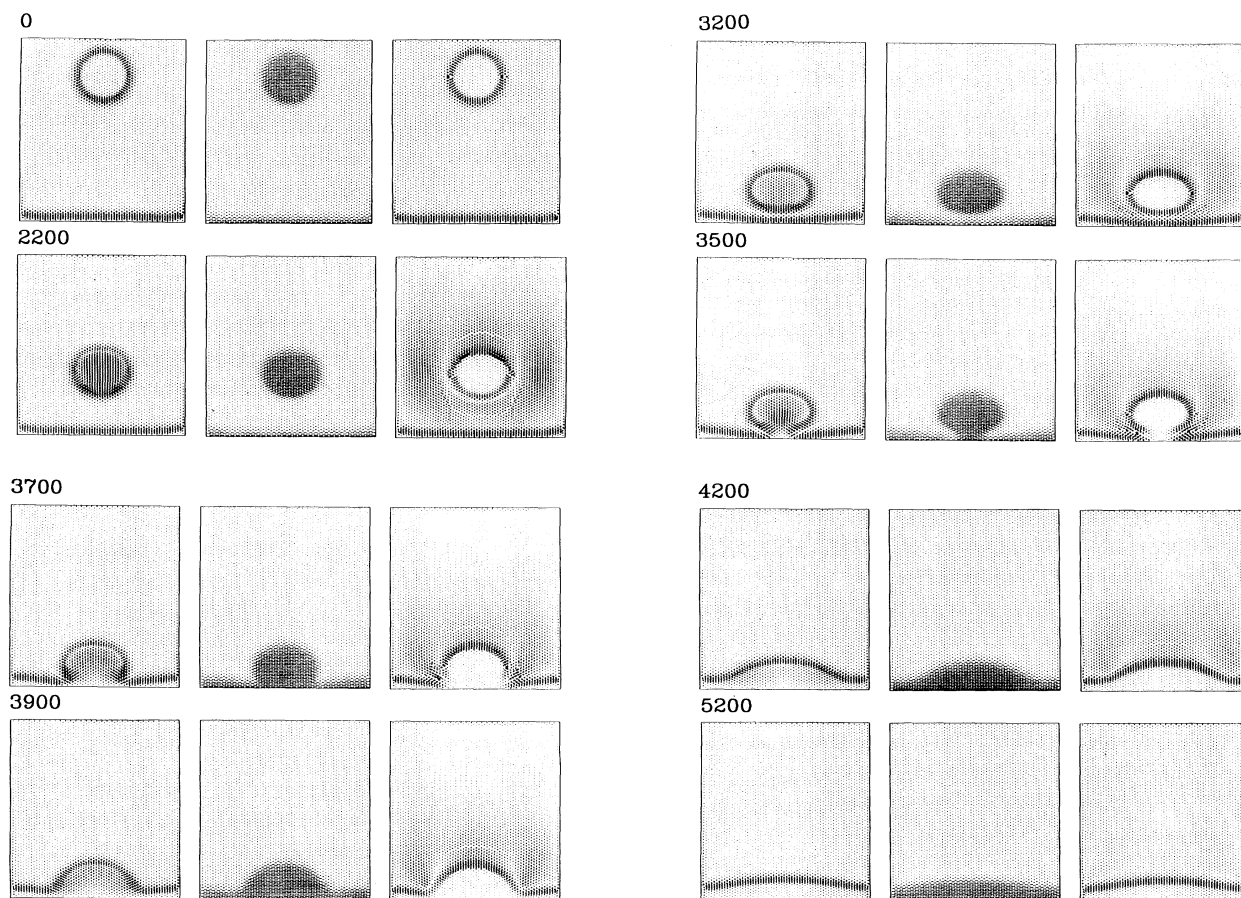


FIG. 7. Coalescence of a red droplet with a shallow red fluid at the bottom of a cavity, as described in the text. The value of g is 0.0005.

whether the direction α is parallel to the field or at an angle, and the sign is picked depending on whether the velocity state is parallel or antiparallel to the field. We show results for two values of g : 0.002 and 0.0005.

We consider three situations for the state of the bottom of the cavity: (a) the bottom wall is red, (b) the bottom wall is red and is covered by a few layers of red fluid, and (c) the bottom wall is red and is covered by many layers of red fluid. It is convenient to start with case (b). What happens here is shown in Figs. 7 and 8 for $g=0.0005$ and 0.002, respectively. The sets of panels are now arranged left to right so that the red momentum is shown on the left and the blue momentum on the right, with the red density in the middle. The numbers indicate time elapsed after the droplet was formed and the gravitational field applied.

The lower value of g , in Fig. 6, brings the droplet to the bottom essentially undistorted. In the immediate vicinity of the bottom fluid the shallow red fluid at the bottom first gets distorted, then merges with the droplet through one connection, and then gradually submerges further. Eventually, the red fluid at the bottom becomes flat. Throughout the process, unlike what happens in rupture, it is the blue momentum that is affected on longer length scales.

This effect becomes even more evident for larger values of g , as shown in Fig. 8. In this case, the droplet gets gravity-distorted before meeting the bottom fluid; it becomes kidney-shaped and the momentum field of the surrounding fluid is affected in a structured and long range fashion. On the impact, two and not one connecting legs are formed, which follows from the initial distortion of the droplet itself. The space between the two legs becomes trapped and an isolated bubble of the blue fluid forms and must now "evaporate." This is done by first making a connecting passage at the top and a gradual filling in of the bubble space.

From now on we consider only $g=0.002$, since this case leads to richer structures. Figure 9 refers to situation (a), no red fluid to the bottom. The physics is similar to that shown in Fig. 7 but the two legs connect to the wall directly. The bubble still forms, but as the trapped space fills in, a much more visible red minidroplet appears above the interface. Thus this process has some elements of splashing.

The most spectacular structures appear when the bottom fluid is deep, as shown in Fig. 10. In the first stage, the bottom fluid is pushed by the droplets momentum and gets heavily distorted. In the second stage, two narrowly separated legs connect the fluid at the bottom and

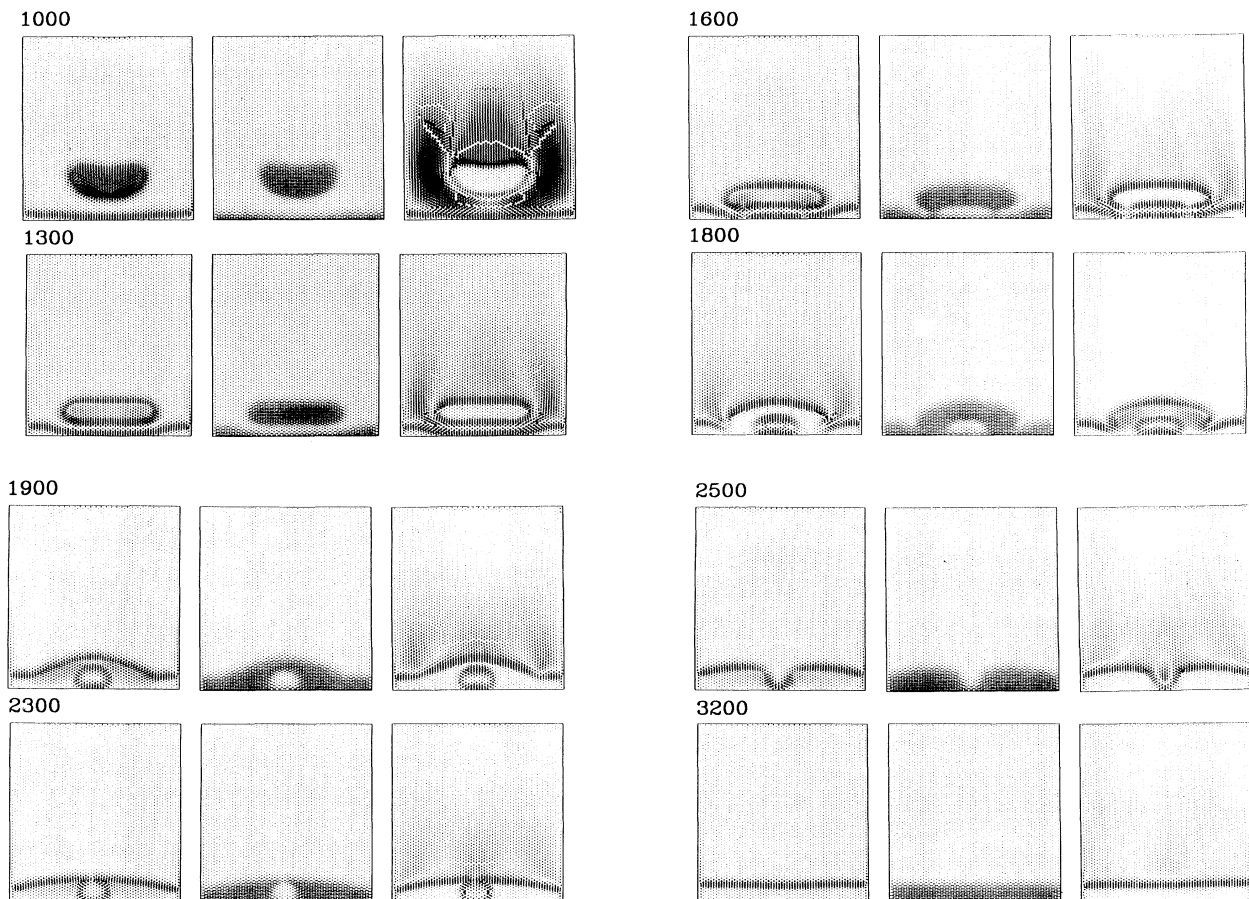


FIG. 8. Same as in Fig. 6 but for $g=0.002$.

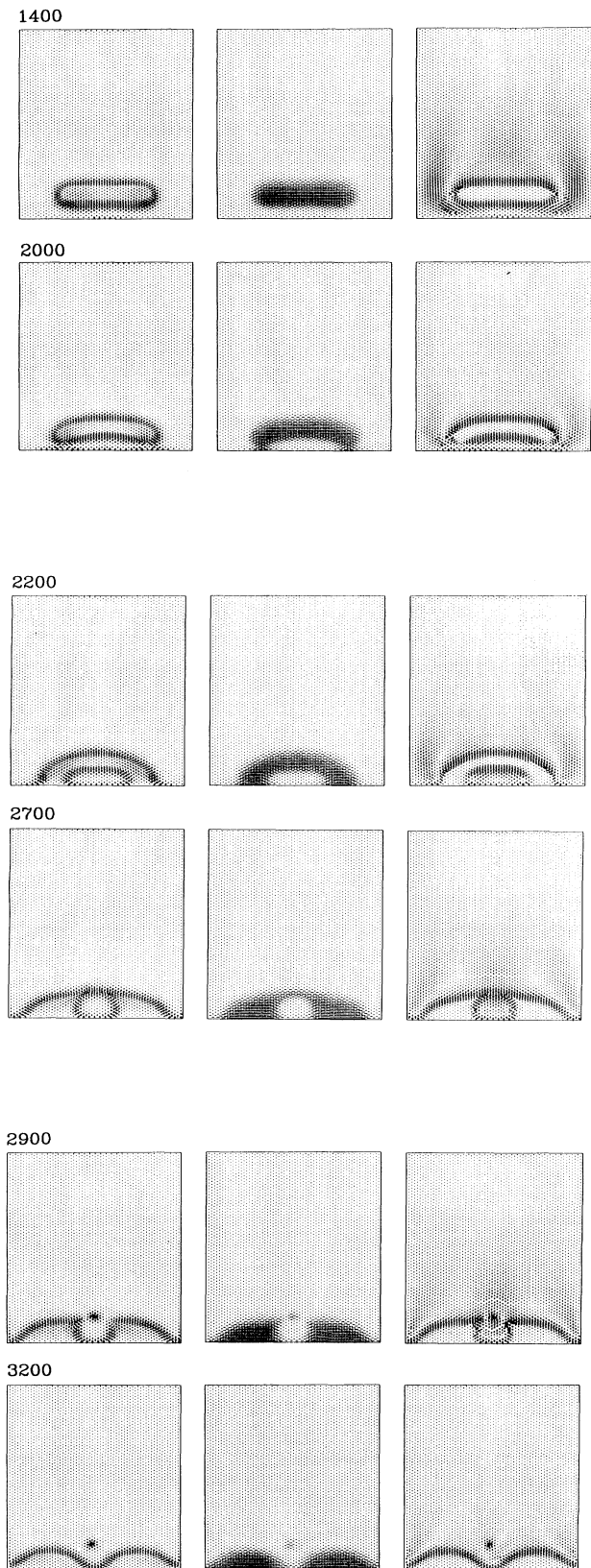


FIG. 9. The fall of a red droplet on a red wall at $g = 0.002$.

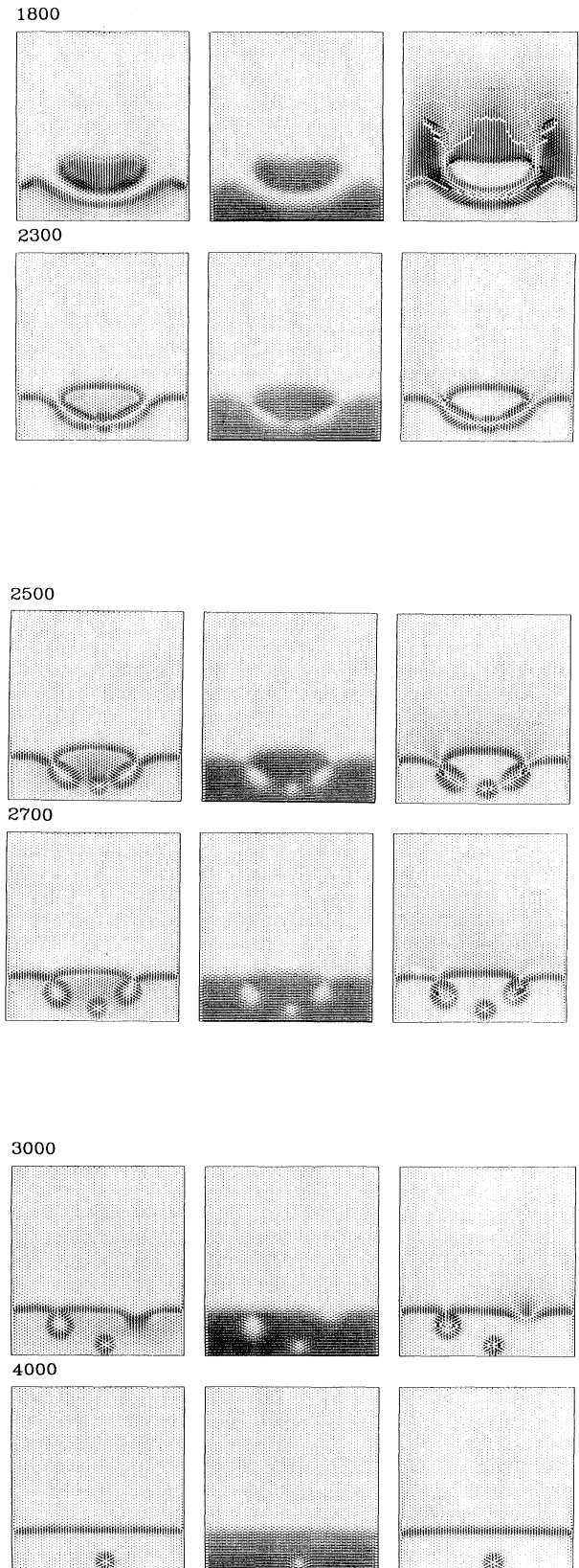


FIG. 10. Coalescence of a red droplet with a deep red fluid at $g = 0.002$.

the droplet. Simultaneously, two side channels on the outsides of the legs are formed. In the next stage, three bubblelike objects are formed. The side bubbles are not identical because the initial droplet was placed close to the center line, and not right on it. Finally, the two side bubbles evaporate, whereas the central bubble remains attached to the wall.

Finally, we note that if the color of the bottom wall were changed to blue, bouncing or splashing would be expected to take place. With the parameters at hand, however, we could merely produce "levitation" of a kidney-shaped droplet over the bottom wall: the gravity pulls the droplet down and the wetting forces keep it up in an equilibrium fashion. Higher values of g , incidentally, give rise to a gravitational rupture of the droplet into subdroplets before impacting on the bottom.

V. CONCLUDING REMARKS

In summary, we have presented systematic studies of rupture and coalescence in a toy kinetic model. The re-

sults on the density and momentum fields are well above the noise level and are hard to obtain otherwise. Systematic trends for the Lyapunov distance in a rupture process have been obtained. It seems worthwhile to continue studies of this model and, in particular, to study droplets falling at an oblique angle, collisions of several droplets, and possible oscillations of the droplet interface on approaching a wall.

ACKNOWLEDGMENTS

Discussions with Jayanth R. Banavar, Iwo Bialynicki-Birula, Joel Koplik, and Mark O. Robbins are appreciated. This work was supported by Grant No. 2-0462-91-01 from the Polish Committee of Scientific Research (KBN); by the Donors of the Petroleum Research Fund administered by the American Chemical Society; by a U.S.-Polish NSF cooperative grant; and by the center for Academic Computing at Pennsylvania State University.

-
- [1] M. Rein, *Fluid Dyn. Res.* **12**, 61 (1993), and references therein; *Dynamics and Instability of Fluid Interfaces*, edited by T. S. Sorensen (Springer, Berlin, 1979).
 - [2] J. Koplik and J. R. Banavar, *Science* **257**, 1664 (1992).
 - [3] J. Koplik and J. R. Banavar, *Phys. Fluids A* **5**, 521 (1993).
 - [4] U. D'Ortona, D. Salin, M. Cieplak, R. B. Rybka, and J. R. Banavar, *Phys. Rev. E* **51**, 3718 (1995); U. D'Ortona, D. Salin, M. Cieplak, and J. R. Banavar, *Europhys. Lett.* **28**, 317 (1994); R. B. Rybka, M. Cieplak, U. D'Ortona, D. Salin, and J. R. Banavar, *Phys. Rev. E* **48**, 757 (1993); R. B. Rybka, M. Cieplak, and D. Salin (unpublished).
 - [5] U. Frisch, D. d'Humières, B. Hasslacher, P. Lallemand, Y. Pomeau, and J.-P. Rivet, *Complex Syst.* **1**, 649 (1987).
 - [6] D. H. Rothman and J. M. Keller, *J. Stat. Phys.* **52**, 1119 (1988); see also D. Burgess, F. Hayot, and W. F. Saam, *Phys. Rev. A* **39**, 4695 (1988).
 - [7] A. K. Gunstensen, D. H. Rothman, S. Zaleski, and G. Zanetti, *Phys. Rev. A* **43**, 4320 (1991), and references therein; see also G. R. McNamara and G. Zanetti, *Phys. Rev. Lett.* **61**, 2332 (1988).
 - [8] A. Gunstensen and D. Rothman, *Physica D* **47**, 53 (1991).
 - [9] U. Frisch, B. Hasslacher, and Y. Pomeau, *Phys. Rev. Lett.* **56**, 1505 (1986).
 - [10] Lord Rayleigh, *Philos. Mag.* **34**, 145 (1892).
 - [11] M. Cieplak, E. D. Smith, and M. O. Robbins, *Science* **265**, 1209 (1994).
 - [12] W. Steele, *Surf. Sci.* **36**, 317 (1973).
 - [13] M. San Miguel, M. Grant, and J. D. Gunton, *Phys. Rev. A* **31**, 1001 (1985).
 - [14] *Cellular Automata and Modelling of Complex Physical Systems*, edited by P. Manneville, N. Boccara, G. Y. Vicchiac, and R. Bideaux (Springer-Verlag, Berlin, 1989).
 - [15] R. Benzi, S. Succi, and M. Vergassola, *Phys. Rep.* **222**, 145 (1992); D. Rothman and S. Zaleski, *J. Phys. (Paris)* **50**, 2161 (1989).